PIBB 生物化学与生物物理进展
Progress in Biochemistry and Biophysics
2014, 41(9): 877~886
www.pibb.ac.cn

Molecular Regions Determining The Voltage-dependence of Inactivation for T-type Calcium Channel $Ca_v3.1$*

HE Bing-Jun[1)**], HU Fen[2)], SHANG Xue-Liang[1)], HAN Li-Xin[1)],
WU Guang-Yan[1)], LI Jun-Ying[2)], SUN Jin-Sheng[3)**]

([1)] *College of Life Sciences, Nankai University, Tianjin* 300071, China; [2)] *School of Physics, Nankai University, Tianjin* 300071, China;
[3)] *Tianjin Key Laboratory of Animal and Plant Resistance, College of Life Sciences, Tianjin Normal University, Tianjin* 300387, China)

Abstract The notable features for inactivation of Ca_v3 channels are fast inactivating rate and strong voltage-dependence. We have investigated the molecular basis for determining the voltage-dependence of inactivation for $Ca_v3.1$, focusing on domain Ⅰ and Ⅱ. We made chimeras between $Ca_v3.1$ and $Ca_v1.2$. Chimeras were expressed in oocytes and currents were recorded by voltage clamp. For domain Ⅰ, replacement of S1～S4 or S5～S6 shifted the steady state inactivation curve significantly. These changes were mainly or partially caused by activation-inactivation coupling, rather than molecular modification. Replacement of domain Ⅱ shifted the inactivation curve significantly and these changes refer to molecular modification, indicating that domain Ⅱ contributed to the voltage-dependence of inactivation for $Ca_v3.1$. Furthermore, both voltage sensor region S1～S4 and pore region S5～S6 in domain Ⅱ were also involved, but Ⅰ-Ⅱ linker has no contribution. In addition, we found that the Ⅰ-Ⅱ linker and S5～S6 in domain Ⅰ contributed strongly to inactivation rate for $Ca_v3.1$, while S1～S4 in domain Ⅰ and Ⅱ was not involved. Taken collectively, our results suggest that domain Ⅱ plays a key role in determining the voltage-dependence of inactivation for $Ca_v3.1$, which was different from the molecular determinants for inactivating rate and for voltage-dependence of activation.

Key words $Ca_v3.1$ calcium channel, voltage-dependence of inactivation, molecular determinant, electrophysiology
DOI: 10.3724/SP.J.1206.2013.00472

Voltage-dependent calcium channels play important roles in a range of cellular processes by regulating calcium influx. The molecular structure of the pore-forming subunit (α_1) of calcium channels has four homologous domains (Ⅰ～Ⅳ), each with 6 transmembrane segments (S1～S6). Calcium channels have been classified into three families (Ca_v1～Ca_v3) according to their electrophysiological characteristic, pharmacology and structure [1–2]. The Ca_v3 family displays T-type current and includes three isoforms, $Ca_v3.1$, $Ca_v3.2$ and $Ca_v3.3$, which are also known as α_{1G}, α_{1H} and α_{1I}, respectively [3–4]. The biophysical properties of Ca_v3 channels are markedly different from those of Ca_v1 and Ca_v2. Ca_v3 channels activate at much more negative potential and are therefore called low-voltage-activated (LVA) channels, while Ca_v1 and Ca_v2 are high-voltage-activated (HVA) channels. The inactivation of Ca_v3 channels is fast, strongly voltage-dependent and Ca^{2+}-independent. In contrast, the inactivation of Ca_v1 channels is Ca^{2+}-dependent, rather than voltage-dependent[1–4].

Calcium channel inactivation is an important intrinsic process that prevents the overload of intracellular calcium and ensures the precision of calcium signals. A number of structure-function studies have been devoted to identifying the molecular basis for calcium channel inactivation. It is proposed, though not fully demonstrated, that the inactivation of

*This work was supported by grants from The National Natural Science Foundation of China (31371974, 31071714) and The Open Fund of Tianjin Key Laboratory of Animal and Plant Resistance.
**Corresponding author.
HE Bing-Jun. Tel: 86-22-23504389, E-mail: hebj@nankai.edu.cn
SUN Jin-Sheng. Tel: 86-22-23766820, E-mail:jinshsun@163.com
Received: April 3, 2014 Accepted: May 26, 2014

HVA calcium channels follows a ball-chain mechanism, where the Ⅰ-Ⅱ linker acts as a hinged lid that docks to the S6 regions and occludes the intracellular side of pore [5–8]. For the Ca_v3 family, several molecular regions have been shown to affect the inactivation rate, including the S4 segments in domain Ⅰ, Ⅱ and Ⅳ [9–10], the S6 in domain Ⅲ [11], the selectivity filter [12–14], the C-terminus [14–16], intracellular linkers between domain Ⅰ and Ⅱ [17–19] or between domain Ⅱ and Ⅲ [20], but not a specific part has been found. The molecular mechanism concerning the voltage-dependent inactivation of Ca_v3 channels is not fully understood.

The two notable features for inactivation of Ca_v3 channels are the fast inactivating rate and strong voltage-dependence. Most of the structure-function studies for Ca_v3 channels focuses on the rate of inactivation, while few reports investigated the molecular basis for the voltage-dependence of inactivation. In the previous work, we have studied the molecular determinants for the voltage-dependence of activation for $Ca_v3.1$ by creating chimeras between $Ca_v3.1$ and $Ca_v1.2$, where we found that domain Ⅰ, Ⅲ and Ⅳ play important roles in determining the voltage-dependence of activation and the effects of domain Ⅰ was due to its S5～S6 region; in contrast, domain Ⅱ contributed to a lesser extent [9, 21]. In the present study, we have investigated the molecular determinants for the voltage-dependence of inactivation for $Ca_v3.1$ with a similar approach. We focused on domain Ⅰ and Ⅱ, because these two domains contribute differently in determining voltage-dependence of activation. Our data showed that domain Ⅱ plays a critical role in determining the voltage-dependence of inactivation, and both its S1～S4 and S5～S6 regions contributed. On the contrary, the entire domain Ⅰ and the linker between domain Ⅰ and Ⅱ (Ⅰ-Ⅱ linker) were not involved. In addition, the Ⅰ-Ⅱ linker, S5～S6 in domain Ⅰ contributed strongly to inactivation rate, while S1～S4 in domain Ⅰ and Ⅱ were not involved.

1 Materials and methods

1.1 Materials

The following Ca_v channel cDNA clones were used: mouse brain $Ca_v3.1$ (α_{1G}), accession AJ012569; rabbit cardiac $Ca_v1.2$ (α_{1C}), accession X15539. Unless stated otherwise, restriction enzymes were purchased from New England Biolabs and Promega. Chemical reagents were obtained from Sigma (St. Louis, MO).

1.2 Construction of Ca^{2+} channel chimeras

All chimeras were made by replacing regions in domains Ⅰ or Ⅱ of $Ca_v3.1$ by the corresponding regions in $Ca_v1.2$ using standard PCR overlap extension method as previously described [9, 22]. In brief, for S1 to S4 region of domain Ⅰ chimera (named Ⅰ-S (1-4)C), residues 81～199 of $Ca_v3.1$ were replaced by residues 154～286 of $Ca_v1.2$; for S5 to S6 region of domain Ⅰ chimera (named Ⅰ-S (5-6)C), residues 200～398 of $Ca_v3.1$ were replaced by residues 287～438 of $Ca_v1.2$. The whole domain Ⅱ chimera (GCGG) was made by replacing residues 399 to 967 of $Ca_v3.1$ with residues 439 to 786 of $Ca_v1.2$; For S1～S4 region of domain Ⅱ chimera (Ⅱ-S(1-4)C), residues 742～856 of $Ca_v3.1$ were replaced by residues 553～672 of $Ca_v1.2$; for S5～S6 region of domain Ⅱ chimera (Ⅱ-S(5-6)C) residues 857～967 of $Ca_v3.1$ were replaced by residues 673～786 of $Ca_v1.2$; for the linker between domain Ⅰ and Ⅱ chimera (Ⅰ-Ⅱ(L)C), residues 399～741 of $Ca_v3.1$ were replaced by residues 439～552 of $Ca_v1.2$. Schematic structures for chimeras are shown in the figures.

The sequences of the chimeras were verified by DNA sequencing. For making RNA, all the chimeras and wild type $Ca_v3.1$ were inserted into high-expression vector pGEM-HEL [9]. $Ca_v3.1$ and chimeric cDNAs were linearized with *Mlu* Ⅰ, Capped cRNAs were synthesised *in vitro* using T7 MEGAscript (Ambion).

1.3 Electrophysiological recording and data analysis

Stage Ⅵ oocytes were prepared from *Xenopus laevis* frogs, using standard techniques [23]. Unless stated otherwise, each oocyte was injected with a volume of 50 nl containing 10～20 ng wild type or chimeric cRNA, and then incubated at 19℃ for 2～4 d in modified Barth's solution (88 mmol/L NaCl, 1 mmol/L KCl, 2.4 mmol/L $NaHCO_3$, 0.82 mmol/L $MgSO_4$, 0.33 mmol/L $Ca(NO_3)_2$, 0.4 mmol/L $CaCl_2$, 7.5 mmol/L Tris-HCl, pH 7.6, 10^4 U/L penicillin, and 10 mg/L streptomysin) [9].

For electrophysiological recording, cells were perfused with barium solution (40 mmol/L $Ba(OH)_2$, 50 mmol/L NaOH, 2 mmol/L KOH and 5 mmol/L HEPES, adjusted to pH 7.4 with methanesulfonic acid). The calcium channel currents (with Ba^{2+} as charge carrier to abolish the Ca^{2+}-dependent inactivation) were measured at 22℃～25℃ by the

two-electrode voltage-clamp technique with a Geneclamp500 amplifier (Axon Instruments) as described previously [9, 21]. To determine the voltage dependence of steady-state inactivation, the currents elicited by a 100 ms test pulse were recorded immediately after a 5000 ms long-lasting pre-pulse at various voltages from the holding potential (−90 mV) in 5 mV increments. The peak amplitude of current was measured and normalized to the maxim value. The normalized peak current (I/I_{max}) was plotted against the voltages of pre-pulse. The steady-state inactivation curve was drawn by fitting mean values to Boltzman equation $1/(1+\exp(V-V_{0.5\ inact})/k_{inact})$, where $V_{0.5inact}$ is the half-inactivation potential and k_{inact} is the slope parameter. For measuring time course of activation and inactivation, the currents were elicited by a series of 500 ms depolarizing pulses every 10 s, from −70 mV to +50 mV in a 10 mV step. The inactivation time courses were fit with a single exponential of time constant τ_{inact}, and activation times were taken as the times from 20% to 80% of maximum current ($t_{20\sim80}$).

Data are given as the mean ± S.E.M., and statistical significance was calculated according to Student's t test with $P < 0.05$ as the significant level.

2 Results

2.1 The roles of molecular regions in domain Ⅰ on voltage dependence of inactivation for $Ca_v3.1$

Wild type $Ca_v3.1$ channels have fast and voltage-dependent inactivation, while $Ca_v1.2$ channels underwent little voltage-dependent inactivation. To investigate the roles of molecular regions in domain Ⅰ on voltage-dependence of inactivation for $Ca_v3.1$, we constructed chimeras by replacing the molecular regions in domain Ⅰ of $Ca_v3.1$ with the corresponding regions of $Ca_v1.2$. The steady-state inactivation for chimeras and for wild type $Ca_v3.1$ were measured when expressed in oocytes, using two-electrode voltage clamp recording with Ba^{2+} as charge carrier.

The current of wild type $Ca_v3.1$ channel was fast inactivating (Figure 1a), and its steady state inactivation curve was shown in Figure 1b, with a

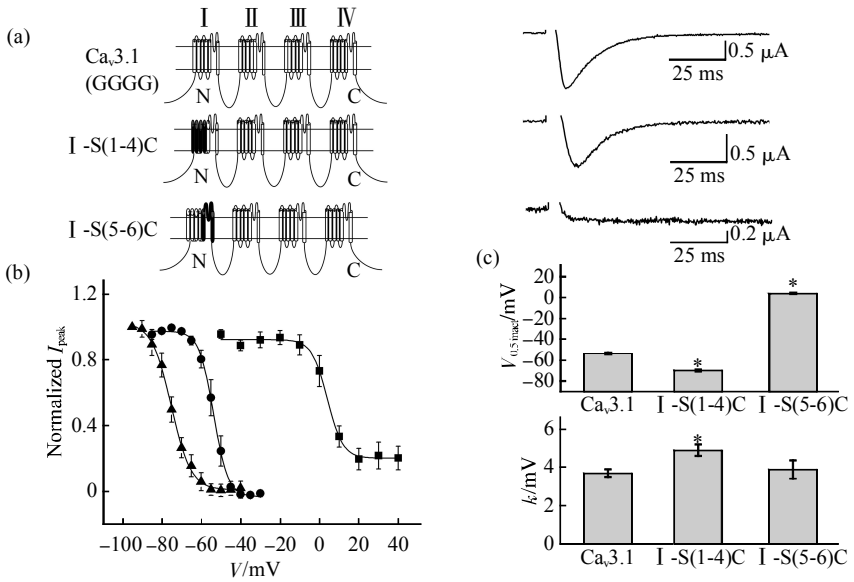

Fig. 1 The roles of S1～S4 and S5～S6 regions in domain Ⅰ on the steady-state inactivation of $Ca_v3.1$

(a) Schematic structures and sample current traces for wild type $Ca_v3.1$ and chimeras. The replaced regions in the chimeras Ⅰ-S(1-4)C and Ⅰ-S(5-6)C were depicted in black. For wild type $Ca_v3.1$, currents elicited by a 100 ms testing pulse of −10 mV, following a 5000 ms long-lasting pre-pulse at various voltages from the holding potential of −90 mV to −30 mV in the steps of 5 mV. Similar protocol of current recording was used in the subsequent figures. Sample current trace at a pre-pulse of −85 mV for $Ca_v3.1$ is shown. For chimera Ⅰ-S(1-4)C, the holding potential was −100 mV, and the testing potential was −30 mV, sample current traces shown were at a pre-pulse of −95 mV. Because Ⅰ-S(5-6)C showed high voltage activated properties, The currents elicited by a 100 ms testing pulse of +20 mV, following a 5000 ms long-lasting pre-pulse at various voltages from the holding potential of −70 mV to +50 mV in the steps of 10 mV. Sample current trace at a pre-pulse of −40 mV for Ⅰ-S(5-6)C is shown. (b) Steady-state inactivation curve for wild type $Ca_v3.1$(●—● , n=8), Ⅰ-S(1-4)C (▲—▲, n=5) and Ⅰ-S(5-6)C (■—■ , n=5). For each individual cell, the peak amplitude of current was measured and normalized to maximum current value. The mean values of normalized currents (I/I_{max}) is plotted against the pre-pulse potential and fitted by the Boltzmann curves. (c) The Boltzmann parameters $V_{0.5\ inact}$ (upper) and k_{inact} (lower). For this, Boltzmann curves were first fitted to each of the steady-state inactivation curves for each individual cell, and then mean values were obtained by averaging $V_{0.5\ inact}$ and k_{inact} over the number of cells. The data are shown as mean ± S.E.M. in this and all subsequent figures; Boltzmann fitting and analysis was also carried out similarly in subsequent figures. *$P < 0.05$ compared with wild type $Ca_v3.1$.

value for its Boltzmann parameters, half-inactivation potential ($V_{0.5\ inact}$) and slope factor ($k_{\ inact}$) of –54 mV and 3.7 respectively(Figure 1c). For chimera Ⅰ-S(1-4)C, which has the S1～S4 region in domain Ⅰ of $Ca_v3.1$ replaced by that of $Ca_v1.2$, the calcium channel currents were fast inactivating (Figure 1a), and the steady state inactivation curve shifted negatively (Figure 1b) with a $V_{0.5\ inact}$ of –70 mV (Figure 1c). For chimera Ⅰ-S(5-6)C, which has the S5～S6 region in domain Ⅰ replaced, the chimeric channel undergo little voltage-dependent inactivation, where the currents inactivated incompletely during test pulse (Figure 1a); Its inactivation curve showed a massive positive shift, (Figure 1b), with a $V_{0.5\ inact}$ of 4 mV (Figure 1c) .

It is known that inactivation can be coupled to activation. Modification in molecular structure may induce correlated changes in voltage-dependence of activation and inactivation; therefore the shifts in inactivation curve may be due to the change in activation, rather than structure modification. In order to exclude putative contamination by activation influence, we calculated and compared the changes in $V_{0.5\ inact}$ with that in half-activation potential ($V_{0.5\ act}$). A ratio value near 1 indicates that shifts in inactivation and activation is parallel, a value near 0 indicates that there is little contamination from activation effects, and a negative value shows the structure modification results in opposite shifts in inactivation and activation. This analysis was carried out in these and the following results, and the values of the changes in $V_{0.5\,inact}$ and $V_{0.5\,act}$ were collected and compared in Figure 4.

For chimera Ⅰ-S(1-4)C, the inactivation curve showed a –16 mV shift, and its activation curve shifted –7 mV (our previously data in reference [21]), so the ratio value for the change in $V_{0.5\ inact}$ to that in $V_{0.5\ act}$ is 2.2, indicating that the negative shift for inactivation curve was partially due to replacement of S1～S4. For chimera Ⅰ-S(5-6)C, the inactivation shifted markedly to the positive direction, however its activation also showed a large positive shift [21], resulting in a ratio value of 1.1 (Figure 1 and Figure 4). This indicated that the shift of inactivation curve was mainly caused by the changes of activation process, rather than replacement of S5～S6. Taken collectively, data shows that the S5～S6 region in domain Ⅰ was not involved in the voltage-dependence of inactivation, and the S1～S4 region did not contribute to some extent.

2.2 The role of domain Ⅱ on voltage dependence of inactivation for $Ca_v3.1$

To investigate the role of domain Ⅱ on voltage-dependent inactivation of $Ca_v3.1$, we replaced the second domain (including the linker between domain Ⅰ and Ⅱ) in $Ca_v3.1$ with the corresponding region in $Ca_v1.2$, forming chimera GCGG (Figure 2a). The calcium currents for chimera GCGG displayed much

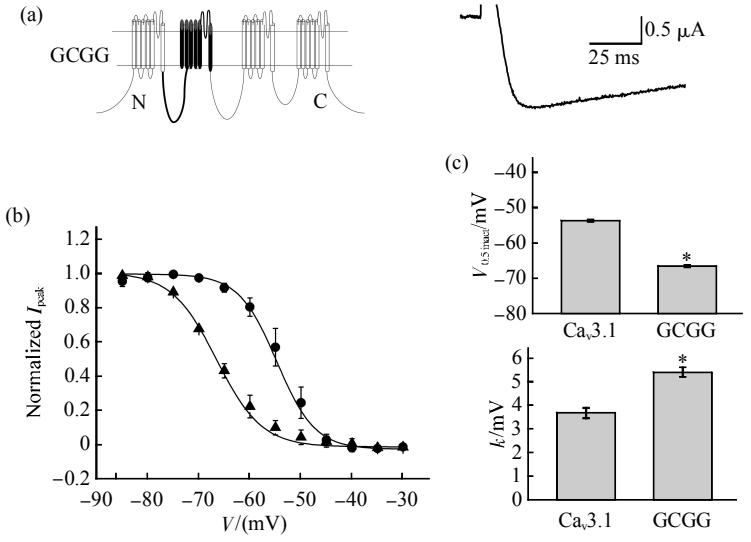

Fig. 2 The role of domain Ⅱ on steady-state inactivation of $Ca_v3.1$

(a) Schematic structures (left) and sample current traces (right) for chimera GCGG. The replaced region in the construction GCGG was depicted in black. The holding potential was –90 mV and testing potential was –10 mV, sample current traces shown were at a pre-pulse of –85 mV. (b) Steady-state inactivation curve for GCGG (▲—▲ , n=5). The mean values of normalized currents (I/I_{max}) is plotted against the pre-pulse potential and fitted by the Boltzmann curves shown, For comparison, steady-state inactivation curve of wild type $Ca_v3.1$ (●—●) is also shown. (c) The Boltzmann parameters $V_{0.5\ inact}$ and $k_{\ inact}$ of GCGG in comparison with that of $Ca_v3.1$. * Significant difference ($P < 0.05$) compared with wild type $Ca_v3.1$.

slower inactivating (Figure 2a), and indeed the time course of inactivation of GCGG was notably larger than that of $Ca_v3.1$. The steady state inactivation curve of GCGG showed a negative shift (Figure 2b), with a $V_{0.5\ inact}$ of –67 mV (Figure 2c). Considering activation-inactivation coupling, we previously showed a positive shift for the activation curve [9], therefore chimera GCGG displayed opposite shifting in inactivation against activation (Figure 4). This indicated that the shift of inactivation curve was entirely due to the replacement of domain Ⅱ and that domain Ⅱ (including Ⅰ-Ⅱ linker) strongly contributed to the voltage-dependence of inactivation.

2.3 Roles of molecular regions in domain Ⅱ on voltage-dependence of inactivation

To narrow down which molecular region in domain Ⅱ is important in controlling voltage-dependence of inactivation, we replaced the Ⅰ-Ⅱ linker, S1～S4 and S5～S6 in domain Ⅱ for $Ca_v3.1$ with the corresponding regions for $Ca_v1.2$, forming chimeras Ⅰ-Ⅱ (L)C, Ⅱ-S(1-4)C and Ⅱ-S(5-6)C respectively (Figure 3a).

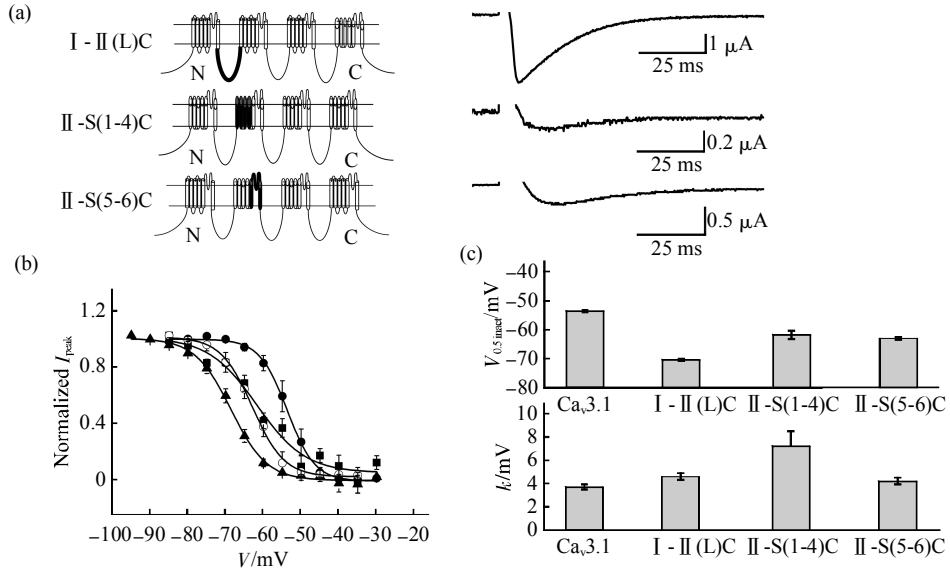

Fig. 3 The roles of Ⅰ-Ⅱ linker, S1～S4 and S5～S6 regions of domain Ⅱ on steady-state inactivation of $Ca_v3.1$

(a) Schematic structures (left) and sample current traces (right) for chimeras. The replaced regions in the constructions were depicted in black. For current recording, the test potential was –30 mV for Ⅰ-Ⅱ (L)C, –10 mV for Ⅱ-S(1-4)C and Ⅱ-S(5-6)C, the holding potential was –100 mV for Ⅰ-Ⅱ (L)C, –90 mV for Ⅱ-S(1-4)C and Ⅱ-S(5-6)C. Sample current traces shown here were at a pre-pulse of –95 mV for Ⅰ-Ⅱ(L)C, –85mV for Ⅱ-S(1-4)C and Ⅱ-S(5-6)C. (b) Steady-state inactivation curves for Ⅰ-Ⅱ (L)C (▲—▲, n=9), Ⅱ-S(1-4)C (■—■, n=4), and Ⅱ-S(5-6)C (○—○, n=5). The mean values of normalized currents (I/I_{max}) is plotted against the pre-pulse potential and fitted by the Boltzmann curves shown, For comparison, steady-state inactivation curve of wild type $Ca_v3.1$ (●—●) is also shown. (c) The Boltzmann parameters $V_{0.5\ inact}$ and k_{inact} for Ⅰ-Ⅱ (L)C (n=9), Ⅱ-S(1-4)C (n=4) and Ⅱ-S(5-6)C (n=5) in comparing with that for wild type $Ca_v3.1$. *P < 0.05.

For Ⅰ-Ⅱ(L)C, the calcium channel currents were fast inactivating (Figure 3a current trace), and its inactivation curve shift negatively, with a $V_{0.5\ inact}$ of –70 mV (Figure 3b and c). We have showed that the activation of Ⅰ-Ⅱ (L)C had a negative shift of –18 mV[21](Figure 4), thus the ratio for the changes in $V_{0.5\ inact}$ to that in $V_{0.5\ act}$ was about 1. This suggests that the shift in the inactivation was caused by the changes in activation, rather than the replacement of Ⅰ-Ⅱ linker, therefore the Ⅰ-Ⅱ linker in $Ca_v3.1$ did not contribute to the voltage-dependence of inactivation.

The calcium currents of chimera Ⅱ-S(1-4)C and Ⅱ-S(5-6)C showed voltage dependent inactivation, but their inactivating rates were slower than that of $Ca_v3.1$ (Figure 3a, current traces). The steady state inactivation curves for both Ⅱ-S(1-4)C and Ⅱ-S(5-6)C shifted negatively, and the $V_{0.5\ inact}$ was –62 mV for Ⅱ-S(1-4)C and –63 mV for Ⅱ-S(5-6)C (Figure 3c). Considering voltage-dependence of activation, we previously showed that activation curves for these two chimeras shifted positively by +18 mV for Ⅱ-S(1-4)C and +25 mV for Ⅱ-S(5-6)C[21]. Thus the steady state

inactivation curves shifted opposite to the activation curves (Figure 4), indicating that the changes in the inactivation curves were entirely due to molecular structure modification. Therefore both S1～S4 and S5～S6 region in domain Ⅱ contributed strongly to the voltage-dependence of inactivation.

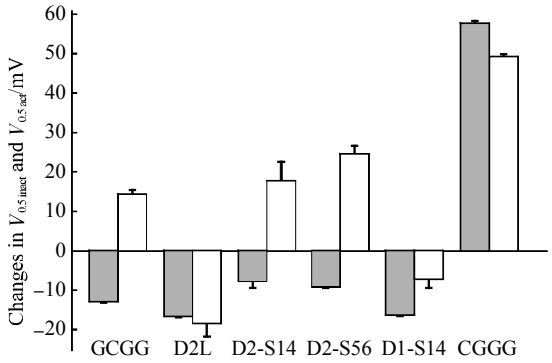

Fig. 4 Comparison of the change of half-inactivation potential ($V_{0.5\,inact}$) with that of half-activation potential ($V_{0.5\,act}$) for each chimera

The data for $V_{0.5\,inact}$ are showing in the figures above, and the data for $V_{0.5\,act}$ are from our previous paper[9, 21]. The changes were obtained by subtracting the mean values for wild type $Ca_v3.1$ from that for chimeras. ■: Inactivation; □: Activation.

2.4 Time course of inactivation

The inactivation time course for chimeras and wild type $Ca_v3.1$ were collected in Figure 5(a, b). To exclude the influence of activation-inactivation coupling, we also measured the time course for activation and presented it in Figure 5c. For each chimera, the changing folds of times at a test potential of 0 mV for inactivation and activation were shown in Figure 5d.

Chimera Ⅰ-S(1-4)C was fast inactivating and the inactivation time course was similar to that of $Ca_v3.1$ (Figure 5b), while chimera Ⅰ-S(5-6)C showed little voltage-dependent inactivation, notably different from wild type $Ca_v3.1$. For activation time courses, these two chimeras were similar to that of $Ca_v3.1$(Figure 5c). These data indicated that S5～S6 region in domain Ⅰ strongly contributed to the inactivation kinetics of $Ca_v3.1$, but S1～S4 region did not.

The inactivating rate of GCGG was greatly slower than that for $Ca_v3.1$ (Figure 5a and sample current trace in Figure 2), and indeed the inactivating times of GCGG at 0 mV were 50-fold larger than that of $Ca_v3.1$; however, the activation times at 0 mV of GCGG were only 4-fold slower than that of $Ca_v3.1$ (Figure 5d), indicating that domain Ⅱ (include the Ⅰ-Ⅱ linker)

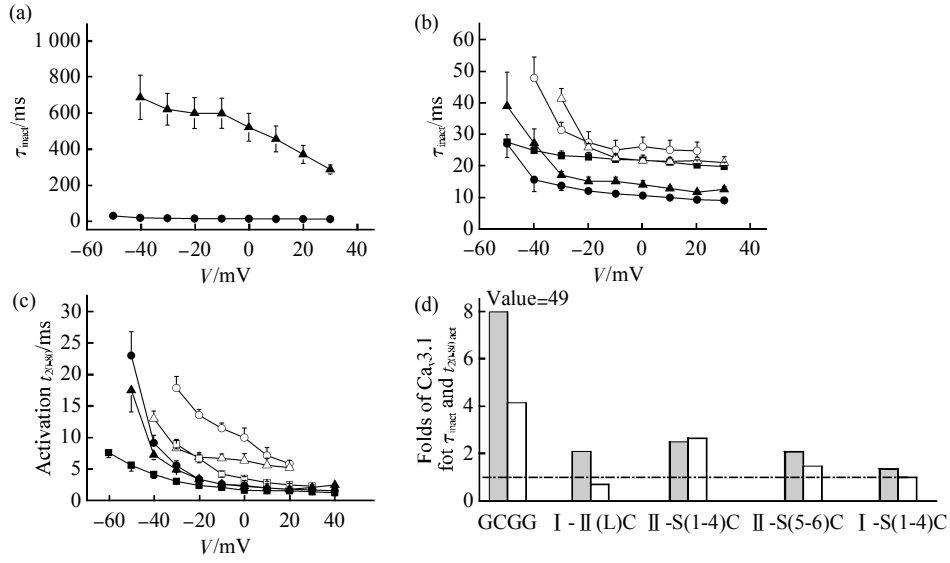

Fig. 5 Time course of inactivation and activation for wild type $Ca_v3.1$ and chimeras

(a) Time course of inactivation, τ_{inact}, for wild type $Ca_v3.1$ (●—●, n=6) and chimera GCGG (▲—▲, n=6) is plotted against the test potential. (b) Time course of inactivation is plotted against the test potential for chimeras Ⅰ-S(1-4)C (▲—▲, n=6), Ⅰ-Ⅱ(L)C (■—■, n=8), Ⅱ-S(1-4)C (○—○, n=4) and Ⅱ-S(5-6)C (△—△, n=5). The inactivation times for wild type $Ca_v3.1$ (●—●) is also shown for comparison. (c) Time course of activation, $t_{20\text{-}80}$, is plotted against the test potential, for wild type $Ca_v3.1$(●—●, n=6), for chimeras Ⅰ-S(1-4)C (▲—▲, n=6), Ⅰ-Ⅱ (L)C (■—■, n=8), GCGG (○—○, n=6), Ⅱ-S(1-4)C (△—△, n=4) and Ⅱ-S(5-6)C (□—□, n=5). (d) Comparison of the changes of inactivation times with that of activation times. For this, the mean value of times for inactivation (shade) and activation (open) at a test potential of 0 mV for each chimeras were divided by that for wild type $Ca_v3.1$, and the fold values are plotted. The dash line shows the value of wild type $Ca_v3.1$. ■:%(τ_{inact}); □: $t_{20\text{-}80\,act}$

was involved in the fast inactivation rate of $Ca_v3.1$. Furthermore, the inactivation rate of chimera Ⅰ-Ⅱ(L)C was about 2- fold slower than that of $Ca_v3.1$ and, its activating time was slightly faster than $Ca_v3.1$ (Figure 5b, c), meaning that the Ⅰ-Ⅱ linker played an important role in determining inactivation rate of $Ca_v3.1$. For chimera Ⅱ-S(1-4)C, both the inactivation and activation times were slower than those of $Ca_v3.1$ with a similar extent (Figure 5d). This indicates the changes in inactivation rate were mostly caused by activation-inactivation coupling, thus the S1～S4 region in domain Ⅱ did not contribute to inactivation rate. For chimera Ⅱ-S(5-6)C, the inactivating and activating times were both larger than those of $Ca_v3.1$; however, the changes of inactivation were somewhat bigger than that of activation, indicating that S5～S6 region in domain Ⅱ contributed to the inactivating kinetics, but to a relatively small extent. Taken together, our data showed that S5～S6 region in domain Ⅰ and the Ⅰ-Ⅱ linker contributed notably to the inactivation rate of $Ca_v3.1$; S5～S6 region in domain Ⅱ had a relatively small contribution; S1～S4 regions in domain Ⅰ and Ⅱ were not involved.

3 Discussion

In the present study, we have investigated the molecular determinants for the voltage-dependence of inactivation of $Ca_v3.1$, focusing on domain Ⅰ and domain Ⅱ, because these two domains play different roles in channel opening. Domain Ⅰ of $Ca_v3.1$ plays a critical role in determining voltage-dependence of activation, and this is due to its S5～S6, rather than S1～S4 region[9, 21]. One may expect that domain Ⅰ, in particular S5～S6 region, might also contribute to the voltage-dependence of inactivation. Surprisingly, our data showed that the replacement of S1～S4 or S5～S6 region in domain Ⅰ shifted steady state inactivation curve significantly, however these changes were mainly (for S5～S6) or partially (for S1～S4) caused by activation-inactivation coupling, rather than molecular structure modification. We also tested chimera CGGG, in which the whole domain Ⅰ was replaced, and the case for CGGG was similar to that for chimera Ⅰ-S(5-6)C (data not show). These results indicated that domain Ⅰ was not involved in the voltage-dependence of inactivation of $Ca_v3.1$, though S1～S4 region contributed to some extent. Unlike domain Ⅰ, domain Ⅱ is less important for voltage-dependence of activation[9]. We showed in the present work that replacement of domain Ⅱ (including Ⅰ-Ⅱ linker) in $Ca_v3.1$ shifted the inactivation curve significantly in a direction opposite to that of activation, indicating that domain Ⅱ contributed notably to the voltage-dependence of inactivation. We further investigated which molecular region was responsible for this contribution, and found that the transmembrane region S1～S6 in domain Ⅱ, rather than Ⅰ-Ⅱ linker was involved. These results above suggest that the molecular determinants for voltage-dependence of inactivation of $Ca_v3.1$ were different from those for activation: domain Ⅱ play a key role in inactivation, although it was less important for activation; On the contrary, domain Ⅰ, which contributed strongly to activation, did not guide the voltage-dependence of inactivation.

There are some structure-function studies for T-type channel inactivation. However, most of these studies are focused on the fast inactivating rate. With respect to the inactivation of Ca_v3 family, several molecular regions have been shown to affect the inactivation rate, including the S4 segments in domain Ⅰ, Ⅱ and Ⅳ[9–10], the S6 in domain Ⅲ[11], the selectivity filter[12–14], the C-terminus[14–16], intracellular linkers between domain Ⅰ and Ⅱ[17–19] or between domain Ⅱ and Ⅲ[20], but no specific part has been found. Although these molecular regions have been implicated in the inactivation mechanism of Ca_v3 channels, to our knowledge, there are few reports investigating the detailed molecular basis for the voltage-dependent inactivation of Ca_v3 channels. Staes *et al.*[15] (2001) have found that replacement of C-terminus or Ⅲ-Ⅳ linker in $Ca_v3.1$ with the corresponding region in $Ca_v3.1$ shifted the $V_{0.5inact}$ significantly, however they did not examine the changes in $V_{0.5act}$, therefore it can not exclude the probability that the shift in $V_{0.5inact}$ was due to activation-inactivation coupling, rather than structure modification. Lee[24–25] group has investigated the structural elements for inactivating rate for $Ca_v3.3$ by making chimera between $Ca_v3.1$ and Cav3.3. Although these chimeras showed some shifts in steady state inactivation curves, these changes were mostly due to activation-inactivation coupling, rather than molecular modification. It is interesting to compare the results for $Ca_v3.1$ with other types of voltage-gated ion channels. For HVA calcium channels $Ca_v2.2$ (a 1E), each four domain in $Ca_v2.2$ contributed differently in controlling the voltage-dependence of inactivation, where domain

Ⅱ and Ⅲ were more important [26]. For the sodium channel, which has a similar molecular structure formed from four homologous domains Ⅰ to Ⅳ, each four domain did not contribute equally to voltage-dependent properties: domain Ⅰ, Ⅱ and Ⅲ involved in activation, domain Ⅳ strongly contributed to inactivation [27-29]. Our results in the present study suggest that T-type calcium channel may have some similarities with sodium channel. We did not test the contributions of domain Ⅲ and Ⅳ in the present work. Since effects of these two domains on activation were similar to domain Ⅰ, their roles on inactivation may have some similarities. Further work is needed to test this deduction.

In the present study, we also examined the inactivation rate for chimeric channels, and more precisely, excluded the influence of activation-inactivation coupling by comparing the changes in activating and inactivating times. Our data showed that S5～S6 in domain Ⅰ and the Ⅰ-Ⅱ linker contributed strongly to the inactivating rate of $Ca_v3.1$, despite their unimportant roles in voltage-dependence of inactivation. In contrast, the S1～S6 region in domain Ⅱ had slight effects on inactivating rate, although this region was critical for voltage-dependence. These results suggest that the voltage-dependence and rate of inactivation for $Ca_v3.1$ were determined by different molecular structures. It has been reported that, for HVA calcium channel, the key regions for inactivation rate were Ⅰ-Ⅱ linker, S6 in domain Ⅱ and Ⅲ. However these regions do not control the voltage-dependence of inactivation [6]. Our results for $Ca_v3.1$ were consistent with their observations.

The linker between domain Ⅰ and domain Ⅱ is one of the key elements controlling inactivation rate for both HVA and T-type calcium channels. Moreover, in all three Ca_v3 channels, Ⅰ-Ⅱ linker serves as a gating brake governing channel opening [17-19, 30-31]. For the voltage-dependence of inactivation, our data in the present work and other reports [17-19] showed that structure modifications in Ⅰ-Ⅱ linker shifted the voltage-dependence of inactivation to the same direction with a similar extent as that for activation, suggesting that Ⅰ-Ⅱ linker did not contribute to the voltage-dependence of inactivation. The pore region, in particular S6 segment, is important for inactivation rate of both T-Type [9, 32] and HVA calcium channels[5-7]. Here we showed that the pore region in domain Ⅰ did indeed strongly contribute to inactivation rate, however the pore region in domain Ⅱ was not involved. One possible explanation for this may be that the S5～S6 in domain Ⅱ is responsible for determining the voltage-dependence, rather than kinetics of inactivation, once again confirming the conclusion that different molecular regions have distinct roles in determining channel functional process.

In summary, our present work shows that the S1～S6 region in domain Ⅱ play an important role in determining voltage-dependence of inactivation for $Ca_v3.1$, whereas domain Ⅰ and Ⅰ-Ⅱ linker are not involved. The contributions of these regions to voltage-dependence of inactivation are different from those of activation. This suggests that the voltage-dependence of activation and inactivation is governed by different molecular structures. In addition, the Ⅰ-Ⅱ linker, S5～S6 in domain Ⅰ contributed strongly to inactivation rate, while S1～S4 in domain Ⅰ and Ⅱ was not involved. This data suggests that molecular determinants for voltage-dependence and rate of inactivation are distinct.

Acknowledgements We thank Gloria Andolina for critical review of the manuscript.

References

[1] Catterall W A. Structure and function of voltage-gated ion channels. Ann Rev Biochem, 1995, **64**: 493-531

[2] Hofmann F, Lacinova L, Klugbauer N. Voltage-dependent calcium channels: from structure to function. Rev Physiol Biochem and Pharmacol, 1999, **139**: 33-87

[3] Perez-Reyes E. Molecular physiology of low-voltage-activated T-type calcium channels. Physiol Rev, 2003, **83**(1): 117-161

[4] Iftinca M C, Zamponi G W. Regulation of neuronal T-type calcium channels. Trends Pharmacol Sci, 2009, **30**(1): 32-40

[5] Stotz S C, Jarvis S E, Zamponi G W. Functional roles of cytoplasmic loops and pore lining transmembrane helices in the voltage-dependent inactivation of HVA calcium channels. J Physiol, 2004, **554**(2): 263-273

[6] Stotz S C, Hamid J, Spaetgens R L, et al. Fast inactivation of voltage-dependent calcium channels. A hinged-lid mechanism?. J Biol Chem, 2000, **275**(32): 24575-24582

[7] Stotz S C, Zamponi G W. Identification of inactivation determinants in the domain IIS6 region of high voltage-activated calcium channels. J Biol Chem, 2001, **276**(35): 33001-33010

[8] Stotz S C, Zamponi G W. Structural determinants of fast inactivation of high voltage-activated Ca^{2+} channels. Trends Neurosci, 2001, **24**(3): 176-181

[9] Li J, Stevens L, Klugbauer N, *et al*. Roles of molecular regions in

determining differences between voltage dependence of activation of $Ca_v3.1$ and $Ca_v1.2$ calcium channels. J Biol Chem, 2004, **279**(26): 26858−26867

[10] Lam A D, Chikina M D, McNulty M M, *et al*. Role of Domain IV/S4 outermost arginines in gating of T-type calcium channels. Pflugers Arch, 2005, **451**(2): 349−361

[11] Marksteiner R, Schurr P, Berjukow S, *et al*. Inactivation determinants in segment IIIS6 of Ca(v)3.1. J Physiol, 2001, **537**(1): 27−34

[12] Talavera K, Janssens A, Klugbauer N, *et al*. Pore structure influences gating properties of the T-type Ca^{2+} channel alpha1G. J Gen Physiol, 2003, **121**(6): 529−540

[13] Talavera K, Staes M, Janssens A, *et al*. Aspartate residues of the Glu-Glu-Asp-Asp (EEDD) pore locus control selectivity and permeation of the T-type Ca^{2+} channel alpha (1G). J Biol Chem, 2001, **276**(49): 45628−45635

[14] Talavera K, Nilius B. Biophysics and structure-function relationship of T-type Ca^{2+} channels. Cell Calcium, 2006, **40**(2): 97−114

[15] Staes M, Talavera K, Klugbauer N, *et al*. The amino side of the C-terminus determines fast inactivation of the T-type calcium channel alpha1 G. J Physiol, 2001, **530**(1): 35−45

[16] Murbartián J, Arias J M, Perez-Reyes E. Functional impact of alternative splicing of human T-type Ca (v)3.3 calcium channels. J Neurophysiol, 2004, **92**(6): 3399−3407

[17] Arias-Olguín II, Vitko I, Fortuna M, *et al*. Characterization of the gating brake in the Ⅰ-Ⅱ loop of Ca (v)3.2 T-type Ca^{2+} channels. J Biol Chem, 2008, **283**(13): 8136−8144

[18] Baumgart J P, Vitko I, Bidaud I, *et al*. Ⅰ-Ⅱ loop structural determinants in the gating and surface expression of low voltage-activated calcium channels. PLoS One, 2008, **3**(8): e2976

[19] Shcheglovitov A, Vitko I, Bidaud I, *et al*. Alternative splicing within the Ⅰ-Ⅱ loop controls surface expression of T-type Ca (v) 3.1 calcium channels. FEBS Lett, 2008, **582**(27): 3765−3770

[20] Chemin J, Monteil A, Bourinet E, *et al*. Alternatively spliced alpha (1G) ($Ca_v3.1$) intracellular loops promote specific T-type Ca^{2+} channel gating properties. Biophys J, 2001, **80**(3): 1238−1250

[21] Li J, Stevens L, Wray D. Molecular regions underlying the activation of low-and high-voltage activating calcium channels. Eur Biophys J, 2005, **34**(8): 1017−1029

[22] Ho S N, Hunt H D, Horton R M, *et al*. Site-directed mutagenesis by overlap extension using the polymerase chain reaction. Gene, 1989, **77**(1): 51−59

[23] Jiang L H, Gawler D J, Hodson N, *et al*. Regulation of cloned cardiac L-type calcium channels by cGMP-dependent protein kinase. J Biol Chem, 2000, **275**(9): 6135−6143

[24] Kang H W, Park J Y, Lee J H. Distinct contributions of different structural regions to the current kinetics of the $Ca_v3.3$ T-type Ca^{2+} channel. Biochim Biophys Acta, 2008, **1778**(12): 2740−2748

[25] Park J Y, Kang H W, Jeong S W, *et al*. Multiple structural elements contribute to the slow kinetics of the $Ca_v3.3$ T-type channel. J Biol Chem, 2004, **279**(21): 21707−21713

[26] Spaetgens R L, Zamponi G W. Multiple structural domains contribute to voltage-dependent inactivation of rat brain alpha (1E) calcium channels. J Biol Chem, 1999, **274**(32): 22428−22436

[27] Cha A, Ruben P C, George A L Jr, *et al*. Voltage sensors in domains Ⅲ and Ⅳ, but not Ⅰ and Ⅱ, are immobilized by Na^+ channel fast inactivation. Neuron, 1999, **22**(1): 73−87

[28] Chanda B, Bezanilla F. Tracking voltage-dependent conformational changes in skeletal muscle sodium channel during activation. J Gen Physiol, 2002, **120**(5): 629−645

[29] Chanda B, Asamoah O K, Bezanilla F. Coupling interactions between voltage sensors of the sodium channel as revealed by site-specific measurements. J Gen Physiol, 2004, **123**(3): 217−230

[30] Karmažínová M, Baumgart J P, Perez-Reyes E, *et al*. The voltage dependence of gating currents of the neuronal Ca(v)3.3 channel is determined by the gating brake in the Ⅰ-Ⅱ loop. Pflugers Arch, 2011, **461**(4): 461−468

[31] Perez-Reyes E. Characterization of the gating brake in the Ⅰ-Ⅱ loop of Ca(v)3 T-type calcium channels. Channels, 2010, **4**(6): 453

[32] Talavera K, Nilius B. Evidence for common structural determinants of activation and inactivation in T-type Ca^{2+} channels. Pflugers Arch, 2006, **453**(2): 189−201

调控 T 型钙通道 $Ca_v3.1$ 电压依赖性失活的分子结构域 *

贺秉军[1)**]　胡　芬[2)]　商学良[1)]　韩丽鑫[1)]　吴广彦[1)]　李俊英[2)]　孙金生[3)**]

([1)]南开大学生命科学学院，天津 300071；[2)]南开大学物理学院，天津 300071；
[3)]天津师范大学生命科学学院，天津市动植物抗性重点实验室，天津 300387)

摘要　T 型钙通道(Ca_v3)广泛分布于各类细胞，其显著的电生理学特点是低电位激活和快速的电压依赖性失活．失活在通道的生理功能调节中起十分重要的作用，但具体参与通道失活的分子基础目前并不完全清楚．为明确 $Ca_v3.1$ 通道中调控电压依赖性失活的结构域，用 $Ca_v1.2$ 通道(无电压依赖性失活)结构域Ⅰ和Ⅱ中的 S1～S4、S5～S6 区及Ⅰ和Ⅱ间的联系区替换 $Ca_v3.1$ 中的相应区域，构建嵌合通道，并在卵母细胞中表达，用电压钳技术分析通道的电生理学特性．结果表明，替换Ⅰ中的 S1～S4 或 S5～S6 区可使 $Ca_v3.1$ 的失活特性显著改变，但这种改变主要是由激活 - 失活偶联所致．Ⅱ的替换使通道的失活曲线参数发生显著改变，表明结构域Ⅱ，包括 S1～S4 和 S5～S6 均参与 $Ca_v3.1$ 失活过程的调控．Ⅰ、Ⅱ间的联系区及Ⅰ中的 S5～S6 主要调控 $Ca_v3.1$ 的失活速率，Ⅰ和Ⅱ中的 S1～S4 对通道失活速率无影响．综上所述，结构域Ⅱ是调控 $Ca_v3.1$ 电压依赖性失活的关键因素，结构域Ⅰ不参与该通道失活过程的调控．Ⅰ、Ⅱ间的联系区及Ⅰ中的 S5～S6 主要调控 $Ca_v3.1$ 通道的失活速率，Ⅰ、Ⅱ中的 S1～S4 对通道失活速率无影响．

关键词　T 型钙通道 $Ca_v3.1$，电压依赖性失活，结构域，电生理
学科分类号　Q4，Q6　　**DOI**: 10.3724/SP.J.1206.2013.00472

* 国家自然科学基金资助项目(31071714，31371974)，天津市动植物抗性重点实验室开放基金资助项目．
** 通讯联系人．
贺秉军．Tel: 022-23504389, E-mail: hebj@nankai.edu.cn
孙金生．Tel: 022-23766820, E-mail: jinshsun@163.com
收稿日期：2014-04-03，接受日期：2014-05-26